The FASEB Journal article fj.13-236216. Published online October 17, 2013.

CXXC5 is a transcriptional activator of *Flk-1* and mediates bone morphogenic protein-induced endothelial cell differentiation and vessel formation

Hyun-Yi Kim,[*,†] Dong-Hwa Yang,[*,†,1] Song-Weon Shin,[*,†] Mi-Yeon Kim,[*,†] Jae-Hyun Yoon,[‡] Suhyun Kim,[§] Hae-Chul Park,[§] Dong Woo Kang,[*,‖] DoSik Min,[*,‖] Man-Wook Hur,[‡] and Kang-Yell Choi[*,†,2]

*Translational Research Center for Protein Function Control, [†]Department of Biotechnology, College of Life Science and Biotechnology, and [‡]Department of Biochemistry and Molecular Biology, College of Medicine, Yonsei University, Seoul, South Korea; [§]Graduate School of Medicine, Korea University, Ansan, South Korea; and [‖]Department of Molecular Biology, College of Natural Science, Pusan National University, Pusan, South Korea

ABSTRACT **CXXC5 is a member of a small subset of proteins containing CXXC-type zinc-finger domain. Here, we show that CXXC5 is a transcription factor activating *Flk-1*, a receptor for vascular endothelial growth factor. CXXC5 and Flk-1 were accmulated in nucli and membrane of mouse embryonic stem cells (mESCs), respectively, during their endothelial differentiation. CXXC5 overexpression induced *Flk-1* transcription in both endothelium-differentiated mESCs and human umbilical vein endothelial cells (HUVECs). *In vitro* DNA binding assay showed direct interaction of CXXC5 on the *Flk-1* promoter region, and mutation on its DNA-binding motif abolished transcriptional activity. We showed that bone morphorgeneic protein 4 (BMP4) induced *CXXC5* transcription in the cells, and inhibitors of BMP signaling suppressed the *CXXC5* induction and the consequent *Flk-1* induction by BMP4 treatment. *CXXC5* knockdown resulted in suppression of BMP4-induced stress fiber formation (56.8±1.3% decrease, $P<0.05$) and migration (54.6±1.9% decrease, $P<0.05$) in HUVECs. The *in vivo* roles of CXXC5 in BMP-signaling-specific vascular development and angiogenesis were shown by specific defect of caudal vein plex vessel formation (57.9±11.8% decrease, $P<0.05$) in *cxxc5* morpholino-injected zebrafish embryos and by supression of BMP4-induced angigogensis in subcutaneously injected Matrigel plugs in *CXXC5*$^{-/-}$ mice. Overall, CXXC5 is a transcriptional activator for *Flk-1*, mediating BMP signaling for differentiation and migration of endothelial cell and vessel formation.—Kim, H.-Y., Yang, D.-H., Shin, S.-W., Kim, M.-Y., Yoon, J.-H., Kim, S., Park, H.-C., Kang, D. W., Min, D., Hur, M.-W., Choi, K.-Y. CXXC5 is a transcriptional activator of *Flk-1* and mediates bone morphogenic protein-induced endothelial cell differentiation and vessel formation. *FASEB J.* 28, 000–000 (2014). www.fasebj.org**

Key Words: HUVECs · mouse embryonic stem cells · caudal vein plex vessel formation

FLK-1, ALSO CALLED VASCULAR endothelial growth factor receptor 2 (VEGFR2), is the first endothelial receptor to be identified in endothelial precursor cells, which has essential roles in the differentiation of endothelial cells, angiogenesis, and embryonic vascular development (1). Flk-1 is expressed primarily in endothelial cells and is an early marker for endothelial progenitor cells during the endothelial differentiation of embryonic stem cells (ESCs; ref. 2). Flk-1 is important for vessel formation and development of vascular-related organs, and *Flk-1*-deficient mice die around embryonic day 9.5 (3). Thus, Flk-1 should be regulated precisely in a spatiotemporal manner to achieve normal vascular development. Several *cis*- and *trans*-factors are known to regulate *Flk-1* transcription in cell-type-specific manners (4). However, upstream signaling pathways and mediators activating *Flk-1* induction are poorly understood (5).

Previous studies showed that bone morphorgeneic proteins (BMPs) are regulators of vascular development and homeostasis (6), and *Flk-1* was indicated as a potential target of the BMP signaling (7–9). For exam-

Abbreviations: BMP, bone morphogenetic protein; CV, caudal vein; CVP, caudal vein plexus; DA, dorsal aorta; DM, dorsomorphin; EMSA, electrophoretic mobility shift assay; ESC, embryonic stem cell; FBS, fetal bovine serum; hpf, hours postfertilization; HUVEC, human umbilical vein endothelial cell; ISA, intersegmental artery; mESC, mouse embryonic stem cell; NLS, nuclear localization signal; PARP, poly-ADP-ribose polymerase; PBS, phosphate-buffered saline; PCV, posterior cardinal vein; PFA, paraformaldehyde; TGF-β, transforming growth factor β; VV, ventral vein

[1] Deceased.

[2] Correspondence: Department of Biotechnology, College of Life Science and Biotechnology, Yonsei University, Seoul, 120-749, South Korea. E-mail: kychoi@yonsei.ac.kr

doi: 10.1096/fj.13-236216

This article includes supplemental data. Please visit *http://www.fasebj.org* to obtain this information.

ple, BMP2 and BMP4 mediate the endothelial differentiation of ESCs (10–12) and regulate endothelial cellular functions. Both noggin and chordin, the antagonists of BMP2 and BMP4, inhibit BMP-mediated angiogenesis during murine development (12). In zebrafish embryos, BMP signaling plays a critical role in specific vessel formation; BMP2 and BMP receptor (BMPR1/2) are specifically involved in the formation of the caudal vein plexus (CVP) but not the formation of intersegmental arteries (ISAs) during early vascular development (13). BMP4 induces the differentiation of ESCs into Flk-1-positive cells in serum-free conditions and is involved in the proliferation and migration of endothelial cells *via* activation of Flk-1 (8, 9). Injection of human *BMP4* mRNA induced Flk-1 expression in zebra fish embryos (7). These studies implicate the relationship between BMP4 and Flk-1; however, detailed mechanisms and mediators for the *Flk-1* regulation by BMP signaling have not been elucidated.

CXXC5, a zinc-finger family protein evolutionarily conserved among vertebrates (14), is a newly identified target of BMP signaling (15). *CXXC5* is a transcriptional target of Wilms tumor 1 (WT1) and is also a negative regulator of the Wnt/β-catenin signaling pathway (16). In addition, CXXC5 localizes in the cytoplasm and interacts with Dishevelled in neural progenitor cells (15). However, CXXC5 has several motifs in the C-terminal region, such as putative nuclear localization signals (NLSs) and CXXC domains that could be involved in DNA interactions, indicating its potential role as a nuclear DNA-binding factor (17–21). In promyelocytic leukemia cells, CXXC5 was observed in the nucleus (20), and a recent study identifies CXXC5 as a hypoxia-induced transcription factor of cytochrome *c* oxidase subunit 4-2 (22). In this study, we characterized CXXC5 as a BMP-induced nuclear transcription factor activating *Flk-1* and further identified its roles in endothelial cell differentiation, migration, and vessel formation. High nuclear expression of CXXC5 during endothelial differentiation in mouse ESCs (mESCs) indicated that CXXC5 acts as a transcription factor mediating endothelial differentiation. Furthermore, in both endothelial-differentiated mESCs and human umbilical vein endothelial cells (HUVECs), overexpression and knockdown of *CXXC5* resulted in an increase and decrease, respectively, in the expression of *Flk-1*. *In vitro* DNA-binding assay and experiments using a putative DNA-binding domain-deleted CXXC5 mutant confirmed the role of CXXC5 as a transcription factor driving *Flk-1* expression. We identified BMP signaling as an upstream pathway for *CXXC5* transcriptional regulation. BMP4 stimulated *Flk-1* induction and cell motility in endothelial cells, whereas the BMP-induced Flk-1 expression and cell mobility were abolished by *CXXC5* knockdown. CXXC5 was expressed in the posterior cardinal vein (PCV) region of zebrafish embryos in early developmental stages, and *CXXC5* knockdown resulted in a specific defect of CVP formation, which is known as a BMP-signaling-specific vessel formation. Finally, a role of CXXC5 in the BMP-induced angiogenesis was revealed by Matrigel plug assay in *CXXC5*$^{-/-}$ mice. These results indicate CXXC5 to be a BMP-signaling-specific mediator for *Flk-1* regulation and *in vitro* and in *vivo* vessel formation.

MATERIALS AND METHODS

Cell culture, transfection, and reporter analysis

mESCs and HUVECs were cultured as described in a previous study (23).The mESCs were maintained on mitomycin C (Sigma, St. Louis, MO, USA)-treated mouse embryonic fibroblast (MEF) feeder cells in knockout Dulbecco's modified Eagle medium (Gibco, Grand Island, NY, USA) supplemented with 15% fetal bovine serum (FBS; Gibco), 1000 U/ml of leukemia inhibitory factor (Esgro; Chemicon International, Temecula, CA, USA), MEM nonessential amino acids (Gibco), and 5×10^{-5} M β-mercaptoethanol (Gibco). For the undifferentiation condition, the mESCs were transferred onto 0.1% gelatin (Sigma)-coated dishes. For endothelial differentiation, mESCs were cultured on mouse collagen IV (BD Biosciences, San Jose, CA, USA)-coated dishes in α-MEM (Gibco) containing 15% FBS and 5×10^{-5} M β-mercaptoethanol for 4 d. For transient transfection, mESCs were grown for 1 d, transfected with the required plasmids using the Lipofectamine Plus reagent, according to the manufacturer's instructions (Invitrogen, Carlsbad, CA, USA), and then further cultured for 3 d in undifferentiation or differentiation medium and harvested. For indicated cases, mESCs and HUVECs were treated with Wnt3a, BMP4, noggin (R&D Systems, Minneapolis, MN, USA), dorsomorphin (DM; Sigma), or transforming growth factor β (TGF-β; Peprotech, Rocky Hill, NJ, USA) after transfection. For reporter analysis, cells were harvested, rinsed in phosphate-buffered saline (PBS; Gibco), and resuspended in reporter lysis buffer (Promega, Madison, WI, USA) for the luciferase assay. Luciferase activities were measured using a FLUOstar Optima plate-reader (BMG Lab Technologies, Offenburg, Germany) and normalized using β-galactosidase activity as an internal control (24).

RT-PCR

Total RNA was extracted from feeder-independent mESCs and HUVECs using the TRIzol reagent (Invitrogen). Reverse transcription was performed with M-MLV reverse transcriptase (Invitrogen). PCR reactions were performed with *Taq*DNA polymerase (Cosmo Genetech, Seoul, Korea) at 94°C for 5 min followed by 25–35 cycles of 94°C for 30 s, 55–58°C for 30 s, and 72°C for 1 min in a System 2700 (Applied Biosystems, Foster City, CA, USA). For mRNA detections, the following pairs of primers were used: *mouse Flk-1*, forward 5′-tgtactgagagatgg-gaacc-3′ and reverse 5′-gtgttgctccttctttcaac-3′; *human Flk-1*, forward 5′-tgatcggaaatgacactggagcct-3′ and reverse 5′-ttcttggtcatcagcccactggat-3′;, *mouse Tie-2*, forward 5′-tctgtggagtcagcttgctccttt-3′ and reverse 5′-tgagggatg-tttcggcatcagaca-3′; *mouse CyclinD1*, forward 5′-tgctgcaaatggaactgcttctgg-3′ and reverse 5′-taccatggagggtgggttggaaat-3′; *mouse c-Myc*, forward 5′-tggtgtctgtggagaagaggcaaa-3′ and reverse 5′-ttggcagctggatagtccttcctt-3′; *mouse HPRT*, forward 5′-cctgctggattacattaaagcact-3′ and reverse 5′-gtcaagggcatat-ccaacaacaaa-3′; *mouse CXXC5*, forward 5′-agcagtttgcacagtccacagaga-3′ and reverse 5′-tggccagtctttcggttcctacaa-3′; *human CXXC5*, forward 5′-atggcggtg-gacaaaagcaac-3′ and reverse 5′-tcactgaaaccaccggaaggc-3′; *mouse CXXC4*, forward 5′-ttcctctccaccttatcccc-3′ and reverse 5′-tctagcgaagtgccaggttt-3′; *hu-*

man CXXC4, forward 5′-ttcctctccaccttatcccc-3′ and reverse 5′-tctagcgaag-tcccaggttt-3′; and *human GAPDH*, forward 5′-aag-gtcggagtcaacggatttggt-3′ and reverse 5′-agtgatggcatggactgtggtcat-3′). All primers were synthesized by Bioneer (Seoul, South Korea).

Western blot analysis

mESCs and HUVECs were grown and treated with Wnt3a, BMP4, noggin, or DM after transfection. After being cultured, cells were harvested and scraped into a microcentrifuge tube. Whole-cell lysates or fractionated lysates were subjected to Western blot analysis as described previously (23). For cell fractionation, the cells were harvested by centrifugation (450 *g*, 5 min), incubated on ice for 15 min in lysis buffer (10 mM HEPES, pH 7.9; 1.5 mM $MgCl_2$; 10m M KCl; 0.01 M DTT; and protease inhibitors) for swelling, and subsequently was mixed with 10% IGEPAL CA-630 (Sigma). This cell lysate was centrifuged (10,000 *g*, 30 s), and the supernatant was saved as cytoplasmic fraction. The resulting cell pellet was resuspended in extract buffer (20 mM HEPES, pH 7.9; 1.5 mM $MgCl_2$; 0.42 M NaCl; 0.2 mM EDTA; 25% glycerol; 0.01 M DTT; and protease inhibitors) and vortex mixed for 15~30 min. This extract was centrifuged (20,000 *g*, 5 min), and the supernatant was saved as the nuclear fraction. Anti-Oct-4, anti-Flk-1, anti-β-catenin (Santa Cruz Biotechnology, Santa Cruz, CA, USA), anti-Lamin A/C (Cell Signaling, Beverly, MA), anti-CXXC5, and anti-β-actin (Abcam, Cambridge, UK) primary antibodies were used, followed by incubation with horseradish peroxidase-conjugated anti-rabbit (Bio-Rad Laboratories, Hercules, CA, USA) or anti-mouse (Cell Signaling) IgG secondary antibodies. Protein bands were visualized with enhanced chemiluminescence (ECL; Amersham Bioscience, Piscataway, NJ, USA) using a luminescent image analyzer (LAS-3000; Fujifilm, Tokyo, Japan).

Plasmids

A 0.9-kb human *CXXC5* cDNA fragment was obtained by PCR using a pair of primers, forward 5′-GCTCTAGACTATGTC-GAGCCTCGGCGGT-3′ and reverse 5′-CGCGGATCCTCACT-GAAAC-CACCGGAAGGC-3′, from a *CXXC5* cDNA clone [GenBank accession no. BC017439; American Type Culture Collection (ATCC), Manassas, VA, USA]. The product was cut with *Xba*I and *Bam*HI and subcloned into the identical site of the pcDNA3.1/myc His(−) A vector (Invitrogen; Myc-CXXC5-pcDNA3.1). The pGEX4T1-CXXC5 construct for GST-CXXC5 fusion protein production was generated by inserting an *Eco*RI- and *Sal*I-restricted 0.9-kb cDNA fragment of the CXXC5 cDNA clone into same sites of pGEX4T1 (Amersham Bioscience). For CXXC5 (Δ250–322), a pair of primers, forward 5′-GCTCTAGACTATGTCGAGCCTCG-GCGGT-3′ and reverse 5′-CGC GGATCCCAGCTCTCCCTG-CATGGG-3′, was used, and for CXXC5 (Δ1–249), a pair of primers, forward 5′-GCTCTAGACCATGCAGGGAGAGCTG-3′ and reverse 5′-CGCGGATCCTCACTGAAACCACCGGAAGGC-3′, was used. By PCR using these primers, 0.9-, 0.7-, and 0.2-kb *CXXC5* mutant fragments were obtained, respectively. All products were cut with *Xba*I and *Bam*HI and subcloned into identical sites of the pcDNA3.1/myc His(−) A, and named Myc-CXXC5 (Δ250–322)-pcDNA3.1 and Myc-CXXC5 (Δ1–249)-pcDNA3.1, respectively. *CXXC5* point mutants (C263/266R, C275/278R) were generated by PCR-based mutagenesis using the following primers: C263/266R, forward 5′-CGGAAACGCCGCGGCAT-GCGCGCGCC-CTGC-3′ and reverse 5′-GCAGGGCGCGCG-CATGCCGCGGCGTTTCCG-3′; C275/278R, forward 5′-CGCATCAACCGCGAGCAGCGCAGCAGTTGT-3′ and reverse 5′-ACAACTGCTGCGCTG-CTCGCGGTTGATGCG. All primers were synthesized by Bioneer. All constructs and mutations were confirmed by nucleotide sequencing. Flk-1-Luc-pGL3 (25) was obtained from Dr. L. Zeng (University of London, London, UK). An shRNA plasmid targeting *CXXC5* (TRCN0000219529) and its backbone plasmid (pLKO.1-puro) were purchased from Sigma. A gene cassette containing internal ribosome entry site and green fluorescence protein coding region was inserted into these 2 plasmids to generate *CXXC5* shRNA vetor and empty shRNA vector, respectively.

Generation of anti-CXXC5 antibody

GST-CXXC5 fusion proteins were overexpressed in *Escherichia coli* BL21(DE3) pLysS cells and transformed with pGEX4T1-CXXC5, and GST-CXXC5 was purified as described previously (26). An anti-CXXC5 antiserum was generated by immunizing a New Zealand White rabbit initially with 1 mg of the purified GST-CXXC5 mixed with 1 ml Freund's complete adjuvant and then subsequently at 2 wk intervals (2nd and 3rd). A week after the 3rd injection, serum was obtained by euthanizing the animal. The anti-CXXC5 antibody was purified from the antiserum as described previously (27).

siRNA and treatment

siRNAs for *mouse CXXC5* (NM_133687; 5′-ACAUCUCCACGUC-CCUAGUTT-3′ and 5′-GAGGAACAUGCUGUUUGUATT-3′) and *human CXXC5* (NP_057547; 5′-CUCAGUGGCAGAU-GACA-CATT-3′ and 5′-GCACCCGUCUUUAGAACCATT-3′) were synthesized (Bioneer) for knockdown of *CXXC5*. A *GFP* siRNA (5′-GCAUCAAGGUGAACUUCAATT-3′; Bioneer) was used as a negative control. siRNAs were transfected into mESCs and HUVECs at a concentration of 100 nM in a 6-well culture plate using the Lipofectamine Plus reagent (Invitrogen). Transfected cells were further cultured for 36 or 72 h before harvest for RT-PCR analysis or tube formation assay.

In vitro tube formation

Growth Factor Reduced Matrigel Matrix (250 μl; BD Biosciences) was added to each well of a 24-well culture plate and allowed to solidify at 37°C for ≥30 min. mESCs at 4 d of differentiation (7×10^4) and HUVECs (3×10^4) were then seeded on the Matrigel-coated wells, cultured at 37°C in a 5% CO_2 atmosphere incubator for 8~24 h, and observed with a light microscope (Eclipse TE2000-U; Nikon, Tokyo, Japan) equipped with a digital CCD camera (Diagnostic Instruments, Sterling Heights, MI, USA) to verify the formation of the capillary-like structures.

Wound healing assay and immunocytochemical analysis

For immunocytochemistry, mESCs and HUVECs were plated on 0.1% gelatin or mouse collagen IV-coated glass coverslips at a density of $0.5\sim0.7\times10^5$ cells/well in a 24-well culture plate. For wound healing assay, a wound was made by scratching the glass using a pipette tip. mESCs were washed with PBS and fixed in 4% paraformaldehyde (PFA) for 30 min at room temperature. Then, cells were washed 3 times with PBS and rendered permeable with 0.1% Triton X-100 in PBS for 30 min. After being washed 3 times with PBS, the cells were incubated with blocking solution (1% BSA and 1% normal goat serum in PBS) for 30 min and incubated with anti-Oct-4, anti-Flk-1, cleaved poly-ADP-ribose polymerase (PARP; Cell Signaling), or anti-CXXC5 antibody in blocking solution at 4°C overnight. Next, the cells were washed 3 times in PBS and incubated with Alexa Fluor 488-conjugated anti-

rabbit IgG or Alexa Fluor 555-conjugated anti-mouse IgG secondary antibody (Invitrogen) at room temperature for 1 h. For cytoskeleton visualization, FITC-conjugated phalloidin (Invitrogen) was treated with the secondary antibodies. Cell nuclei were counterstained by incubating cells in 1 μg/ml DAPI (Boehringer Mannheim, Indianapolis, IN, USA) for 10 min and were then washed extensively in distilled water. Samples that were fluorescently labeled were examined with a Radiance 2100 multiphoton imaging system (Bio-Rad Laboratories) and a LSM510 Meta microscope (Carl Zeiss, Jena, Germany). The number of cells in wounding area was counted as described previously (28).

Zebrafish experiments

Zebrafish embryos were raised and maintained using standard procedures, and developmental stages were determined as described previously (29). At 24 h postfertilization (hpf), embryos were transferred to water with 0.003% 1-phenyl-2-thiourea (PTU; Sigma) to inhibit pigment formation. The zebrafish lines used in the study were wild-type and *Tg(kdrl:EGFP)*^{s843} (30). Morpholino oligonucleotides (MOs) for *cxxc5* (*cxxc5* MOs; 5′-GCTGTCCGCCAGACATGGTCCAGCC-3′) and control MOs (5′-CCTCTTACCTCAGTTACAATTTATA-3′) were purchased from Gene Tools (Corvallis, OR, USA). The MOs were dissolved in 1× Danieau solution at a concentration of 10 mM and were further diluted with distilled water. Morpholino oligonucleotide (10 ng) was injected into 1- to 2-cell-stage embryos. Zebrafish embryos were cleansed and dissected in PBS. Isolated embryos and tissues were fixed in 4% PFA in PBS supplemented with 4% sucrose overnight at 4°C. For whole-mount embryo staining, embryos were washed in 0.8% TritonX-100 in PBS (PBST), transferred to PBST containing methanol, and then stored −20°C until staining. The embryos were permeablized in 1 mg/ml proteinase K in PBST at 25°C for 40 min. The permeabilization was stopped by being washed with PBST, and then the free amines were quenched with 1 M glycine (pH 8.0). Postfixation were done using 4% PFA in PBS for 20 min at room temperature. Blocking was performed using PBST containing 10% goat serum and 1% DMSO for 2 h at room temperature, and then the embryos were incubated with anti-Flk-1 and anti-cleaved caspase 3 (Cell Signaling) antibodies overnight at 4°C. After being washed with PBST, the embryos were incubated with Alexa Fluor 488-conjugated anti-goat IgG and Alexa Fluor 488-conjugated anti-rat IgG overnight at 4°C. The embryos were washed with PBST and then transferred into PBS containing glycerol for visualization. Immunofluorescent images were visualized using an Eclipse TE2000-U fluorescent microscope. For paraffin sectioning, tissues were dehydrated by serial immersion in ethanol, cleared in xylene, and embedded in paraffin. Tissue blocks were sectioned as 4-μm slices using a microtome. Paraffin-preserved tissues were stored at room temperature before sectioning. Sectioned slices were blocked with serum-free protein blocker (Dako, High Wycombe, UK) and stained with anti-CXXC5, anti-cleaved caspase 3, or anti-Flk-1 (BD PharMingen, San Diego, CA, USA) antibody. Alexa Fluor 488-conjugated anti-goat IgG and Alexa Fluor 488-conjugated anti-rat IgG were used as the secondary antibodies. The slices were counterstained with DAPI. Confocal images were obtained using with a Radiance 2100 multiphoton imaging system and a LSM510 Meta microscope. The thickness of PCV of control MO-injected and *cxxc5* MO-injected *Tg(flk-1:EGFP)* zebrafish embryo at 50 hpf was measured from fluorescent microscope images using NIS-Elements software (Nikon). The percentage of ISA- or CVP-containing segments was calculated from control MO-injected and CXXC5 MO-injected *Tg(flk-1:EGFP)* zebrafish embryos at 50 hpf, as described previously (13).

In vivo angiogenesis analysis

The angiogenesis analysis was performed using the Matrigel implant model system in *CXXC5*$^{+/+}$ and *CXXC5*$^{-/-}$ mice, as described previously (31). Growth factor-reduced Matrigel (BD Biosciences) was thawed overnight on ice and mixed with 1 μg/ml BMP4 in combination with noggin. Matrigel (500 μl) was injected subcutaneously into the dorsal surfaces of *CXXC5*$^{+/+}$ and *CXXC5*$^{-/-}$ mice aged 2.5∼3.5 mo. After 14 d, the Matrigel plugs were isolated and fixed in 4% paraformaldehyde/PBS overnight at 4°C. For cryopreservation, implanted Matrigels were immersed through a graded saccharose/PBS series and then were embedded in Tissue-Tek optimal cutting temperature (OCT) compound (Sakura Finetek, Torrance, CA, USA). Cryopreserved tissues were stored at −80°C until sectioning. Sectioned slices were blocked with serum-free protein blocker and stained with anti-CXXC5, anti-cleaved PARP, or anti-PECAM-1 (BD Biosciences) antibody. Alexa Fluor 488-conjugated anti-goat IgG and Alexa Fluor 488-conjugated anti-rat IgG were used as the secondary antibodies. The slices were counterstained with DAPI. Immunofluorescent images were visualized using a Radiance 2100 multiphoton imaging system and a LSM510 Meta microscope.

RESULTS

CXXC5 is induced during the endothelial differentiation of mESCs and stimulates *Flk-1* transcription in differentiated mESCs and HUVECs

To characterize the involvement of CXXC5 in the endothelial differentiation of mESCs, the mRNA and protein levels of *CXXC5* were measured during the differentiation process. The mRNA levels of *CXXC5* were increased significantly, along with those of *Flk-1*, *Flt-1*, and *Tie-2* by endothelial differentiation of mESCs (**Fig. 1*A***). The protein level of CXXC5 was also increased, whereas that of Oct-4, an ESC marker, was decreased following mESC differentiation (Fig. 1*B*). The increases in both CXXC5 and Flk-1 during mESC endothelial differentiation were further confirmed by immunocytochemical analyses. Here, CXXC5 and Flk-1 protein levels were significantly increased and localized to the nucleus and membrane, respectively, in differentiated mESCs (Fig. 1*C*, bottom panels). To investigate the role of CXXC5 in the endothelial differentiation of mESCs, *CXXC5* was transfected, and the mRNA levels of endothelial differentiation markers were monitored in undifferentiated and differentiated mESCs. Following *CXXC5* transfection, the mRNA levels of *Flk-1* increased significantly in differentiated mESCs (Fig. 1*D, E*). However, the induction of *Flk-1* mRNAs by *CXXC5* transfection was not observed in undifferentiated mESCs (Fig. 1*D*). In addition, *Tie-2* mRNA was induced in differentiated mESCs but was not further increased by *CXXC5* transfection (Fig. 1*D*), indicating that CXXC5 specifically induce *Flk-1* transcription. The transcriptional induction of *Flk-1* by *CXXC5* transfection was further confirmed by reporter analyses, in which *Flk-1* promoter activity was dose-dependently and significantly increased by *CXXC5* transfection in differ-

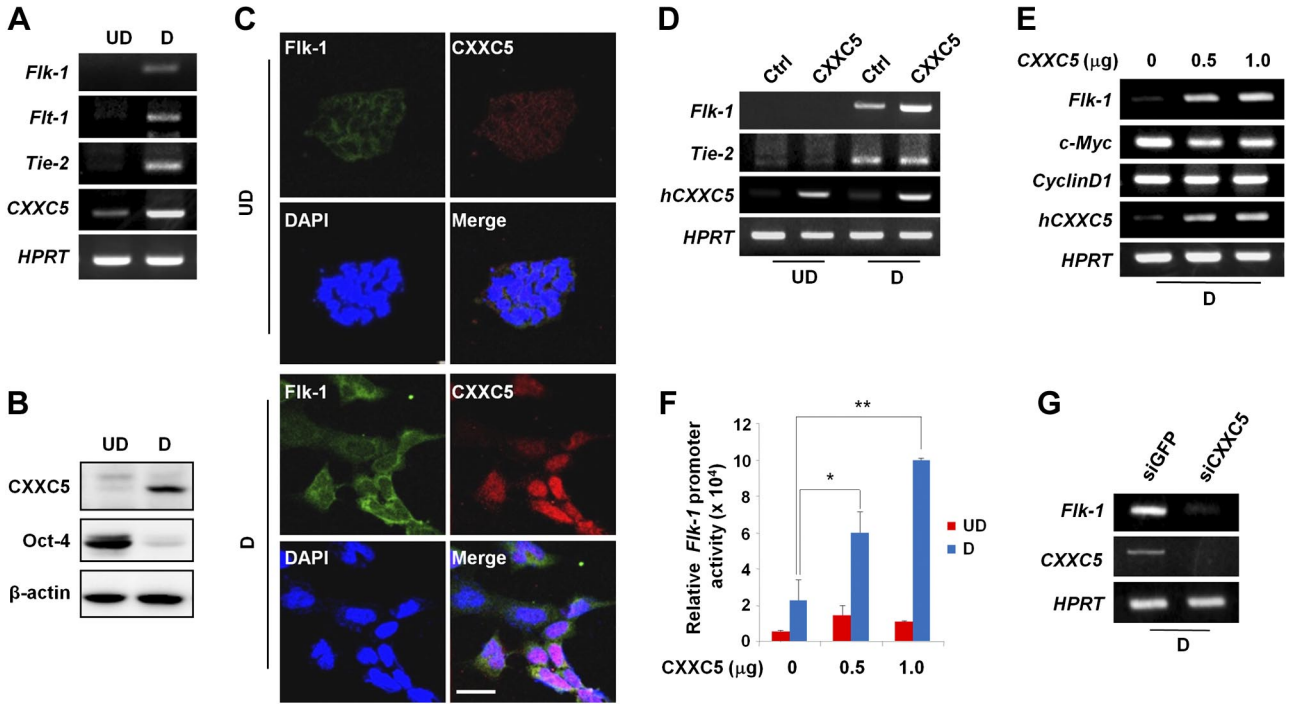

Figure 1. Role of CXXC5 in the transcriptional induction of *Flk-1* during the endothelial differentiation of mESCs. Undifferentiated (UD) or differentiated (D) mESCs grown for 1 d in undifferentiation or differentiation medium were transfected with the pcDNA3.1 control (Ctrl) or Myc-CXXC5-pcDNA3.1 (CXXC5) plasmid (*D*, *E*), or Flk-1-Luc-pGL3 was cotransfected with those (*F*). mESCs were transfected with 100 nM of *GFP* or *CXXC5* siRNA (*G*). Cells were further cultured for 3 d before analyses. *A*, *D*, *E*, *G*) mRNA levels of *Flk-1*, *Tie-2*, *hCXXC5*, *CXXC5*, *c-Myc*, *cyclinD1*, and *HPRT* were detected by RT-PCR analyses. *B*, *C*) Protein levels of Oct-4, CXXC5, Flk-1, and β-actin were detected by Western blot (*B*) or immunocytochemical analyses (*C*). Scale bar = 50 μm. *F*) *Flk-1* promoter reporter analyses were performed as described in Materials and Methods. Error bars = SD of 3 independent reporter analyses. $^*P < 0.05$, $^{**}P < 0.01$.

entiated, but not undifferentiated, mESCs (Fig. 1*F*). As expected, the mRNA level of *Flk-1* was reduced by *CXXC5* knockdown in differentiated mESCs (Fig. 1*G*). Moreover, the level of *Flk-1* mRNA was also increased and decreased as a result of *CXXC5* overexpression and knockdown, respectively, in HUVECs (Supplemental Fig. S1*A*, *B*). The induction of Flk-1 expression by CXXC5 was also demonstrated by the increased Flk-1 protein level in HUVECs transfected with *CXXC5* (Supplemental Fig. S1*C*). However, *Flk-1* mRNA was not altered as a result of transfection with *CXXC4*, an analog of *CXXC5*, in HUVECs (Supplemental Fig. S1*D*), indicating that the transcriptional induction of *Flk-1* in endothelial cells was CXXC5 specific.

CXXC5 is a nuclear transcription factor that induces *Flk-1* expression during the endothelial differentiation of mESCs

The CXXC5 induced during the endothelial differentiation of mESCs was localized primarily within the nucleus (Fig. 1*C*), and the nuclear localization and accumulation of CXXC5 in differentiated mESCs were confirmed by cell fractionation assays (**Fig. 2*A***). The β-catenin level was not reduced by *CXXC5* transfection in either mESCs or HUVECs (Fig. 2*B* and Supplemental Fig. S1*C*), and the mRNA levels of c-*Myc* and *cyclinD1*, both well-known target genes of Wnt/β-catenin pathway (32, 33), also did not decrease on *CXXC5* transfection in differentiated mESCs (Fig. 1*E*). These results imply that CXXC5 functions as a nuclear factor rather than a cytosolic negative regulator of Wnt/β-catenin signaling in endothelial cells.

To identify the functional domains in CXXC5 mediating *Flk-1* regulation, N-terminal and C-terminal deletion mutants, CXXC5 (Δ1–249) and CXXC5 (Δ250–322), were generated (Fig. 2*C*), and the effects of these mutants on the expression of *Flk-1* mRNA were examined. the *Flk-1* mRNA level increased on transfection of the *CXXC5* (Δ1–249) mutant in endothelial-differentiated mESCs (Fig. 2*D*). However, transfection of *CXXC5* (Δ250–322), which lacks the putative CXXC DNA-binding domains (34, 35), did not increase *Flk-1* mRNA (Fig. 2*E*). The loss of function of CXXC5 (Δ250~322) was confirmed by *Flk-1* reporter analyses (Fig. 2*F*). Moreover, both the mRNA level and reporter activity of *Flk-1* decreased on *CXXC5* (Δ250–322) transfection (Fig. 2*E*, *F*). To further confirm the role of the CXXC domains of CXXC5 in *Flk-1* expression, we generated point mutants in which the Cys-263/266 and Cys-275/278 residues were replaced with arginine residues in the first and second CXXC domains, respectively (Fig. 2*C*). Both the mRNA level and promoter activity of *Flk-1* were decreased following transfection with *CXXC5* (C263/266R), as similar with *CXXC5* (Δ250–322) trans-

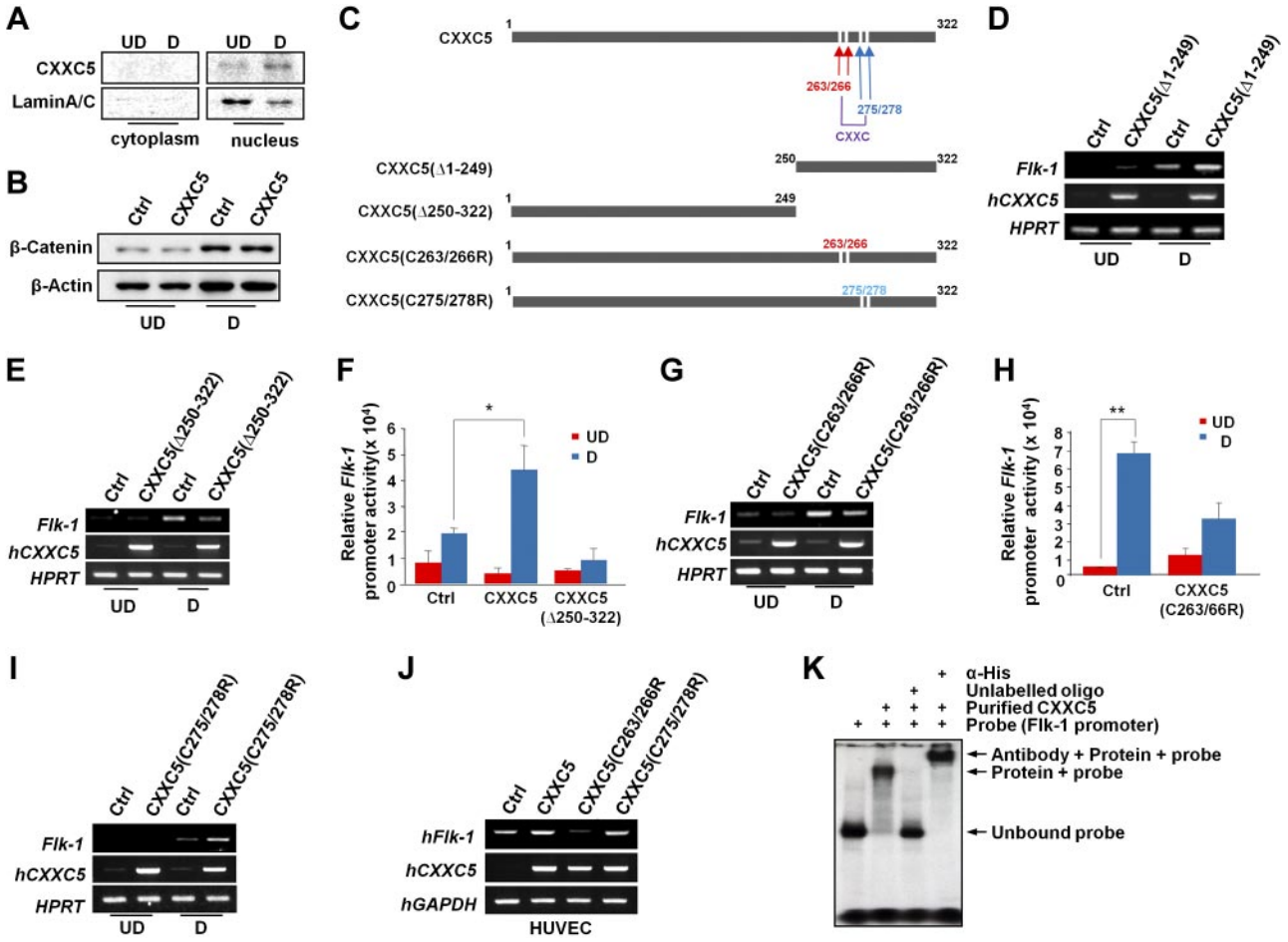

Figure 2. Role of the DNA-binding CXXC domains of CXXC5 in *Flk-1* induction in endothelial-differentiated mESCs and HUVECs. *A*) mESC extracts were separated into nuclear and cytosolic fractions and were then subjected to Western blot analyses to detect CXXC5 and lamin A/C. *B*) mESCs were grown for 1 d in undifferentiation or differentiation medium, and then transfected with pcDNA3.1 or Myc-CXXC5-pcDNA3.1. Cells were further cultured for 3 d and subjected to Western blot analysis to detect the protein levels of β-catenin and β-actin. *C*) Schematic representation of wild-type and mutant CXXC5 proteins. *D–J*) mESCs were grown and transfected with Myc-CXXC5(Δ1–249)-pcDNA3.1 (*D*), Myc-CXXC5(Δ250–322)-pcDNA3.1 (*E, F*), Myc-CXXC5(C263/266R)-pcDNA3.1 (*G, H, J*), Myc-CXXC5(C275/278R)-pcDNA3.1 (*I, J*), or the pcDNA3.1 control, as indicated. Transfected cells were subjected to RT-PCR analyses (*D, E, G, I, J*) to detect mRNA levels of *Flk-1, hCXXC5, hGAPDH*, and *HPRT*, or were subjected to *Flk-1* promoter reporter analyses (*F, H*). Error bars = SD of 3 independent analyses. $*P < 0.05$, $**P < 0.01$. *K*) EMSA using *Flk-1* promoter fragments spanning the −629- to −1-bp region from the transcription start site and recombinant CXXC5 including cold-DNA probe competition and supershift assays using an anti-CXXC5 antibody.

fection, in differentiated mESCs (Fig. 2*G, H*). However, transfection with the *CXXC5* (C275/278R) mutant increased the level of *Flk-1* mRNA in differentiated mESCs (Fig. 2*I*) and also increased *Flk-1* mRNA to wild-type levels in comparison with control in HUVECs (Fig. 2*J*). We further confirmed the reduced, rather than increased, *Flk-1* transcription following *CXXC5* (C263/266R) transfection in HUVECs (Fig. 2*J*). These results indicated that CXXC5 (C263/266R) and CXXC5 (Δ250–322) acted as dominant-negative mutants in terms of their effect on the transcriptional activation of *Flk-1*.

To further confirm the role of CXXC5 as a transcription factor for *Flk-1*, *in vitro* DNA binding assays were performed with purified recombinant CXXC5 and *Flk-1* promoter fragments. CXXC5 interacted with *Flk-1* promoter fragments spanning the −629- to −1-bp region from the transcription start site, as shown by electrophoretic mobility shift assay (EMSA; Fig. 2*K*). Moreover, the specificity of the interaction between CXXC5 and the *Flk-1* promoter DNA fragments was confirmed by the competition of CXXC5-*Flk-1* fragment binding with an unlabeled cold DNA probe and a supershift of the DNA-protein complex with an anti-CXXC5 antibody (Fig. 2*K*). Thus, the first CXXC domain (34, 35) is essential for the role of CXXC5 as a transcriptional activator for *Flk-1*.

CXXC5 mediates the transcriptional induction of *Flk-1 via* BMP4-Smad signaling

BMP4-Smad signaling has been shown to be involved in the differentiation of human ESCs into vascular progenitor cells (36). We found that BMP4 induced both *Flk-1* and *CXXC5* mRNAs in HUVECs (**Fig. 3*A*** and Supplemental Fig. S1*E*). Smad1/5/8 are phosphorylated by BMP-activated receptors to bind with Smad4

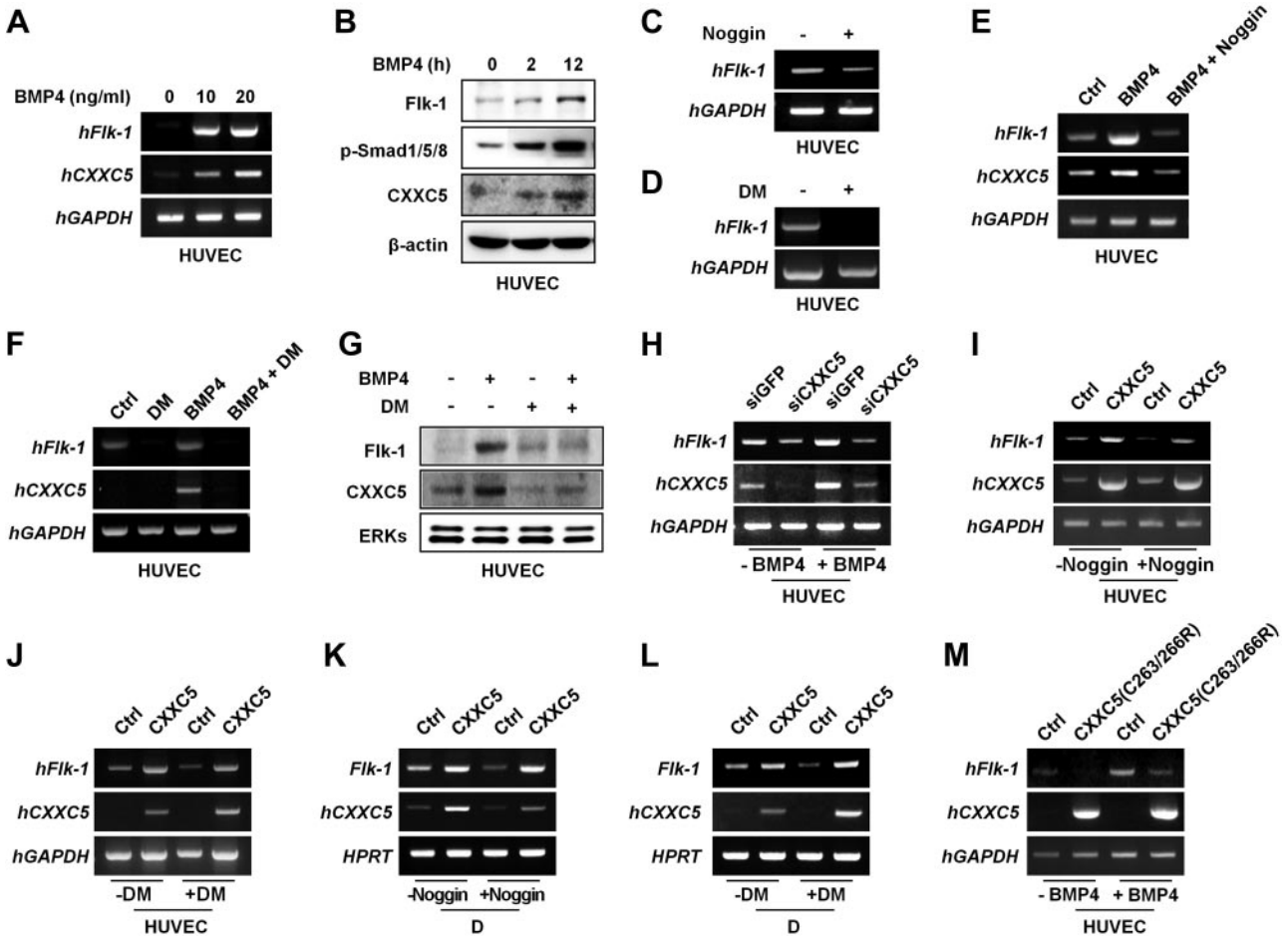

Figure 3. Role of CXXC5 in Flk-1 induction by BMP4 in endothelial differentiated mESCs and HUVECs. *A*) HUVECs were grown for 1 d and treated with BMP4 in serum-free condition for 16 h. *B*) HUVECs were treated with 20 ng/ml BMP4 in serum-free condition for 0, 2, or 12 h. *C, D*) HUVECs were grown for 1 d and treated with 100 ng/ml noggin (*C*) or 10 μM DM (*D*) for 16 h. *E–G*) HUVECs were pretreated with 100 ng/ml noggin (*E*) or 20 μM DM (*F, G*) for 2 h, followed by treatment with 20 ng/ml BMP4 for 16 h. *H*) HUVECs were transfected with *GFP* or *CXXC5* siRNA, and then treated with 20 ng/ml BMP4 in serum-free condition for 16 h. *I, J*) HUVECs were transfected with pcDNA3.1 or Myc-CXXC5-pcDNA3.1 and then treated with 100 ng/ml noggin (*I*) or 20 μM DM (*J*) 1 d after transfection. *K, L*) mESCs were grown in differentiation medium, and transfected with pcDNA3.1 or Myc-CXXC5-pcDNA3.1, as described in Fig. 1*D*, and were then treated with 100 ng/ml noggin (*K*) or 20 μM DM (*L*) for 1 d. *M*) HUVECs were transfected with pcDNA3.1 or Myc-CXXC5(C263/266R)-pcDNA3.1 and then treated with BMP4, as described in panel *A*. Cells were subjected to RT-PCR (*A, C–F, H–M*) or Western blot (*B, G*) analyses.

and translocate into the nucleus to induce target genes (37). With the increase in phosphorylated Smad1/5/8 (p-Smad1/5/8), the protein levels of both Flk-1 and CXXC5 were time dependently increased by BMP4 treatment in HUVECs (Fig. 3*B*). Despite a slight increase in the mRNA level of *Flk-1*, that of *CXXC5* was not altered by Wnt3a treatment (Supplemental Fig. S1*E*). In contrast to the effect of BMP4, treatment with TGF-β, another protein from same family, reduced the mRNA level of *Flk-1* in HUVECs and differentiated mESCs (Supplemental Fig. S1*F, G*), indicating the specificity of BMP4 for the induction of *Flk-1* mRNA.

The basal level of *Flk-1* mRNA was reduced following treatment with noggin, a BMP4 antagonist, and DM, a selective chemical inhibitor of BMP signaling, in HUVECs (Fig. 3*C, D*). *Flk-1* mRNA induction following endothelial differentiation of mESCs was also dose dependently inhibited by noggin and DM (Supplemental Fig. S1*H, I*). Furthermore, the BMP4-induced increase in *Flk-1* mRNA was also blocked by treatment with noggin or DM in HUVECs (Fig. 3*E, F*). Interestingly, the induction of *CXXC5* mRNA by BMP4 was also significantly reduced following treatment with these inhibitors (Fig. 3*E, F*). Down-regulation of the protein level of Flk-1 with p-Smad1/5/8 following DM treatment was also confirmed in HUVECs and differentiated mESCs (Fig. 3*G* and Supplemental Fig. S1*J*). The BMP4-induced *Flk-1* mRNA increase was blocked by *CXXC5* siRNA transfection in HUVECs (Fig. 3*H*), indicating that CXXC5 is a key factor for *Flk-1* mRNA induction by BMP4. To further confirm that CXXC5 functions downstream of the BMP4 signal to induce *Flk-1* transcription, we tested the effect of CXXC5 overexpression in cells treated with noggin or DM. In these HUVECs, CXXC5 induced *Flk-1* mRNA regardless of pretreatment with noggin or DM (Fig. 3*I, J*). In addition, the *Flk-1* mRNA induction by CXXC5 was not affected by noggin or DM in differentiated mESCs (Fig.

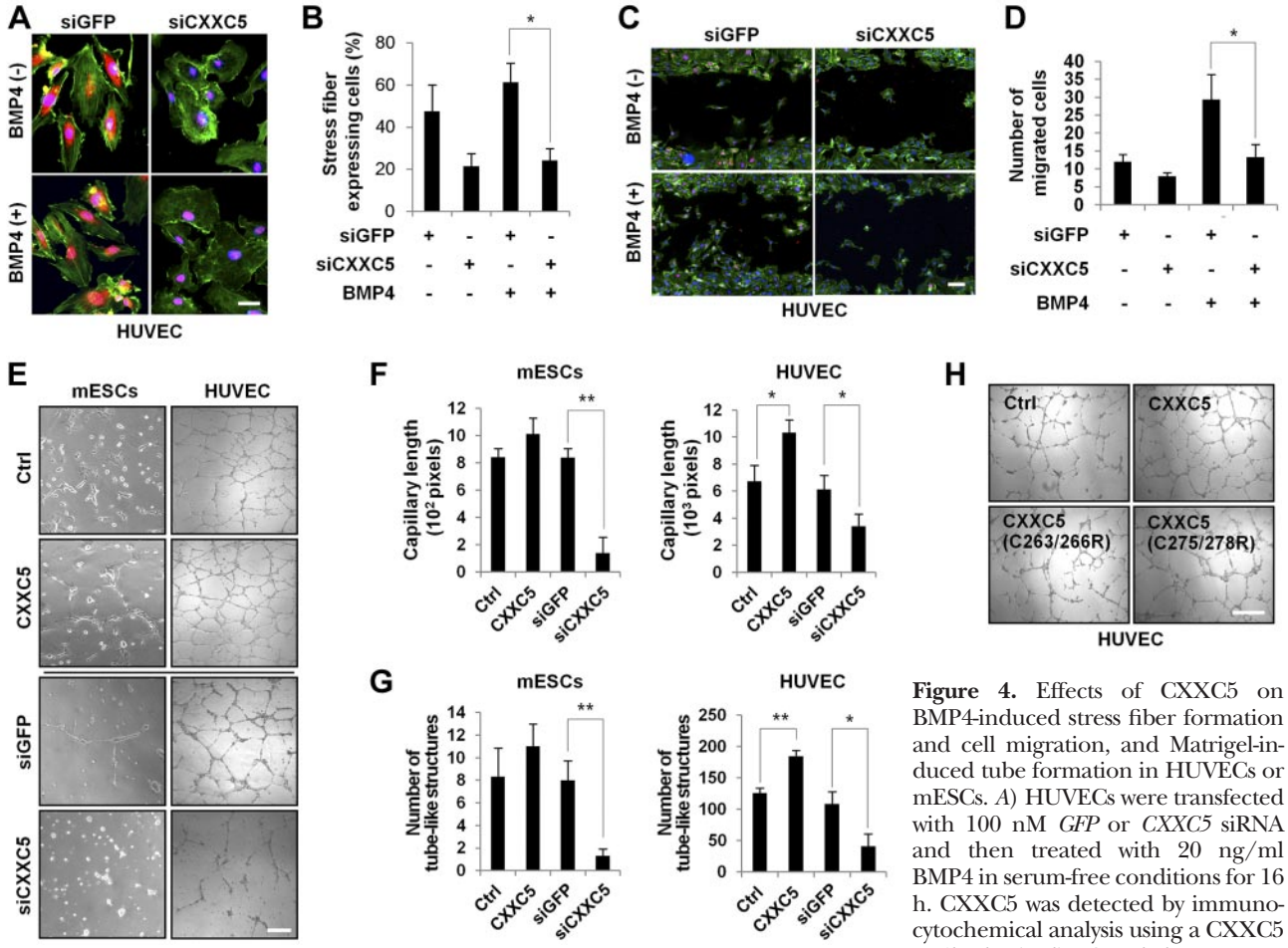

Figure 4. Effects of CXXC5 on BMP4-induced stress fiber formation and cell migration, and Matrigel-induced tube formation in HUVECs or mESCs. *A*) HUVECs were transfected with 100 nM *GFP* or *CXXC5* siRNA and then treated with 20 ng/ml BMP4 in serum-free conditions for 16 h. CXXC5 was detected by immunocytochemical analysis using a CXXC5 antibody (red). Cytoskeletons were visualized using FITC-conjugated phalloidin (green). Nuclei were counterstained with DAPI (blue). Scale bar = 25 μm. *B*) Percentage of cells from panel *A* forming stress fiber. *C*) HUVECs were transfected with 100 nM *GFP* or *CXXC5* siRNA. Wounds were made as described previously (28), and the cells were then treated with 20 ng/ml BMP4 in serum-free conditions for 16 h. Immunocytochemical analysis was performed as described in panel *A*. Scale bar = 100 μm. *D*) Number of cells in the wounded area from panel *C*. *E–H*) mESCs and HUVECs were transferred onto Matrigel-coated plates and transfected with 100 nM *GFP* or *CXXC5* siRNA, or pcDNA3.1, Myc-CXXC5-pcDNA3.1, Myc-CXXC5(C263/266R)-pcDNA3.1, or Myc-CXXC5(C275/278R)-pcDNA3.1. Tube formation was observed after 24 h. Scale bars = 200 μm. Capillary length (*F*) and numbers of tube-like structures (*G*) were calculated as described previously (46, 47). Error bars = SD of 3 independent reporter analyses. $*P < 0.05$, $**P < 0.01$.

3*K*, *L*). However, *Flk-1* mRNA induction by BMP4 was reduced following overexpression of a dominant-negative mutant, CXXC5 (C263/266R), in HUVECs (Fig. 3*M*). Overexpression of inhibitory Smads, Smad6 and Smad7 (38), reduced *Flk-1* mRNA level in both differentiated mESCs and HUVECs (Supplemental Fig S1*K*, *L*). These results indicate that CXXC5 functions downstream of BMP4 signaling to mediate BMP4-induced transcriptional activation of *Flk-1* in endothelial cells and endothelium-differentiated mESCs.

CXXC5 plays a role in BMP4-induced motility and tube formation in endothelial cells

BMP2 treatment or overexpression of BMP endothelial cell precursor-derived regulator (BMPER), an agonist of BMP4, has been shown to induce stress fiber formation and cell motility (39, 40). We found that BMP4 treatment also increased the number of cells forming stress fibers in HUVECs (**Fig. 4*A, B*** and Supplemental Fig. S2*A*). Transfection of *CXXC5* siRNA reduced the number of stress fiber-forming cells to below the basal level, regardless of BMP4 treatment (Fig. 4*B*). In addition, the numbers of migrated cells increased following BMP4 treatment, and the number also decreased on *CXXC5* knockdown (Fig. 4*C*, *D* and Supplemental Fig. S2*B*). Interestingly, CXXC5 was highly expressed in cells showing high mobility (Supplemental Fig. S2*B*).

To characterize the role of CXXC5 in vascularization, the effects of CXXC5 on the formation of tube-like structures were investigated. Total capillary length and the number of tube-like structures in both differentiated mESCs and HUVECs on Matrigel increased on *CXXC5* transfection (Fig. 4*E–G*). In contrast, the total capillary length and number of tube-like structures of these cells decreased following the transfection of *CXXC5* siRNA (Fig. 4*E–G*). Furthermore, overexpres-

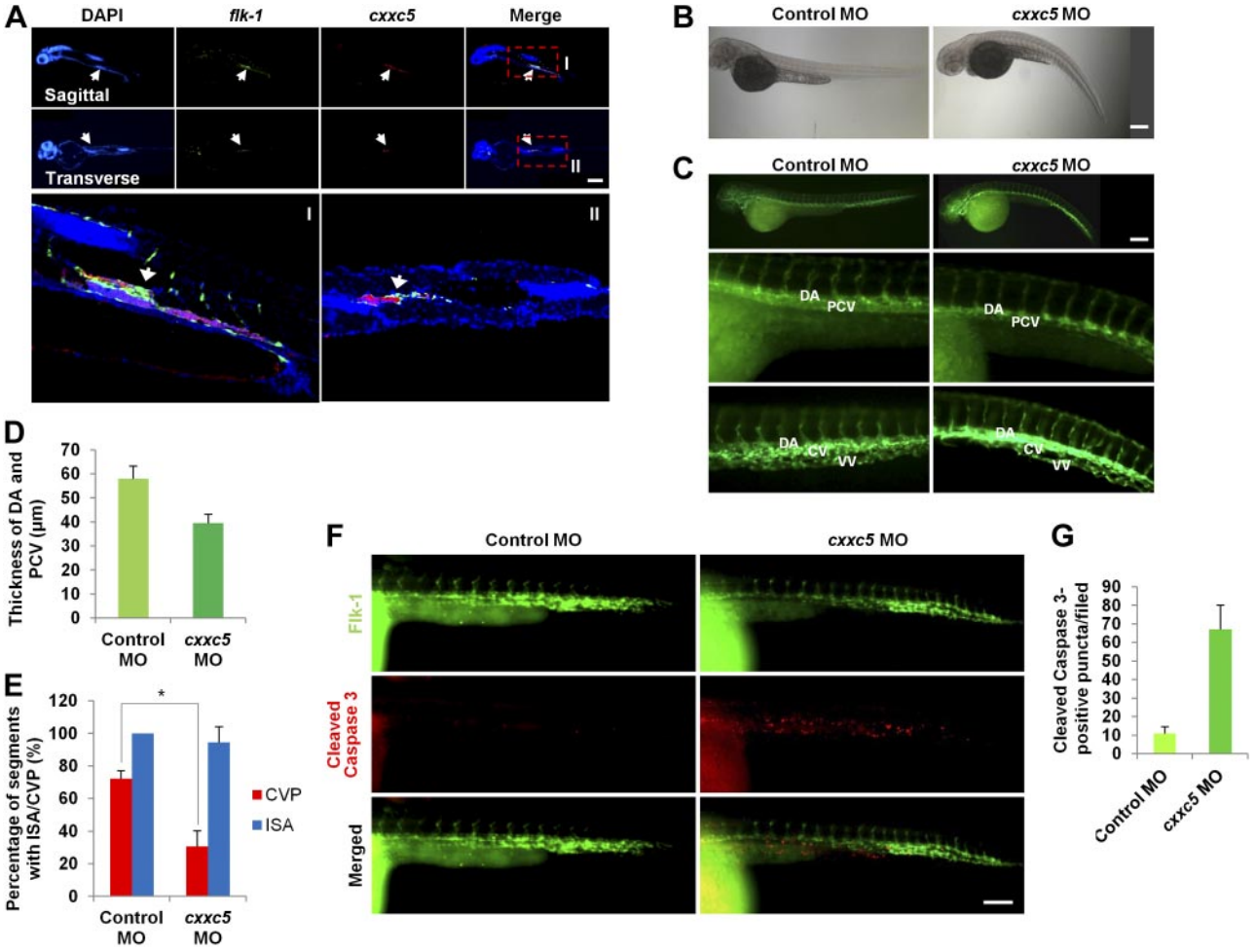

Figure 5. Effect of CXXC5 knockdown on vessel formation in zebrafish embryos. *A*) Sagittal and transverse sections of *Tg(flk-1:EGFP)* zebrafish embryo at 50 hpf were subjected to immunohistochemical analysis to visualize CXXC5. Nuclei were counterstained using DAPI. Scale bar = 200 μm. *B, C*) Bright-field (*B*) and fluorescence (*C*) images of control MO-injected and CXXC5 MO-injected *Tg(flk-1:EGFP)* zebrafish embryos at 50 hpf. Scale bar = 200 μm. *D*) Thickness of the PCV in control MO-injected and CXXC5 MO-injected *Tg(flk-1:EGFP)* zebrafish embryo at 50 hpf. *E*) Percentage of segments containing ISAs or CVP was calculated for control MO-injected and CXXC5 MO-injected *Tg(flk-1:EGFP)* zebrafish embryos at 50 hpf as described previously (13). *F, G*) Control MO-injected and CXXC5 MO injected *Tg(flk-1:EGFP)* zebrafish embryos at 50 hpf were subjected to whole-mount immunohistochemical analyses to visualize cleaved caspase 3 (*F*). Scale bar =100 μm. Numbers of cleaved caspase 3-positive puncta were counted. Error bars = SD of 3 independent reporter analyses (*G*). $*P < 0.05$.

sion of CXXC5 (C263/266R), a dominant-negative mutant, reduced the formation of vascular-like structures, whereas overexpression of CXXC5 or CXXC5 (C275/278R) increased this formation (Fig. 4*H*). These results indicate that CXXC5 mediates BMP4-induced cell motility and *in vitro* tube formation of endothelial cells.

CXXC5 is required for axial vein angiogenesis during zebrafish development

BMP signaling mediates sprouting angiogenesis from the PCV to form the CVP during early vascular development in zebrafish (13). The inhibition of BMP signaling in early zebrafish embryos results in aberrant CVP formation; the dorsal aorta (DA) and the caudal vein (CV) are incompletely separated, and the number of fused ventral vein (VV) decrease without any effect on ISA formation (13). *cxxc5* was specifically expressed in the PCV region of zebrafish embryo at 50 hpf, as confirmed by immunofluorescent labeling of the sagittal, transverse, and coronal sections of *Tg(flk-1:EGFP)* zebrafish embryos (**Fig. 5*A*** and Supplemental Fig. S3*A*, arrows). The immunofluorescence was abolished by preblocking of the sections with purified CXXC5, which confirms the specificity of anti-CXXC5 antibody (Supplemental Fig. S3*B*). The *Tg(flk-1:EGFP)* embryos at 50 hpf that were injected with *cxxc5* morpholinos demonstrated downward-curved body phenotypes (Fig. 5*B*) and aberrant PCV and CVP formation (Fig. 5*C*). The thickness of the PCV was reduced in embryos injected with *cxxc5* morpholinos compared with those injected with control morpholinos (Fig. 5*C*, middle panels; *D*; and Supplemental Fig. S3*C*). The DA and CV separation was incomplete, and the number of fused VVs was decreased in the CVP region of embryos injected with *cxxc5* morpholinos (Fig.

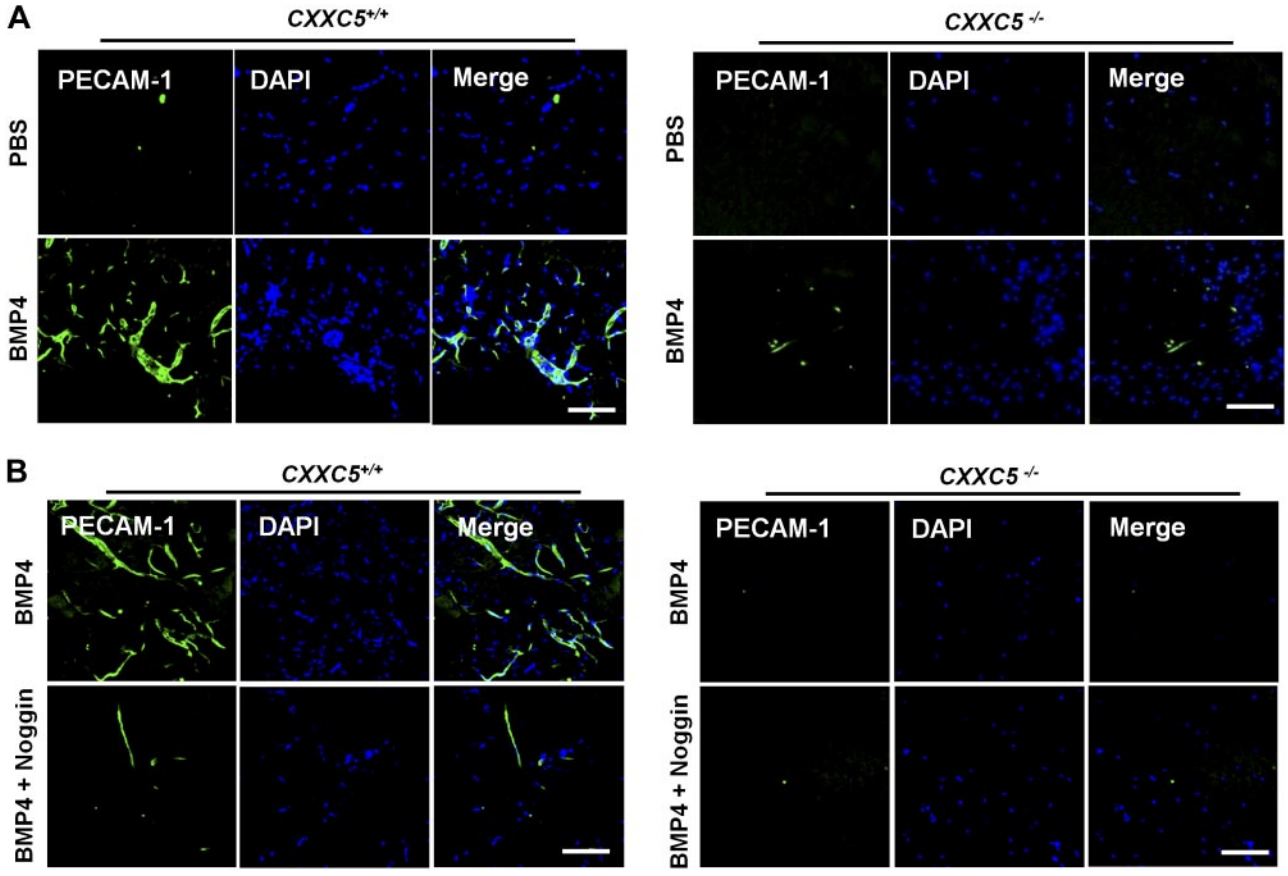

Figure 6. Effects of *CXXC5* knockout on BMP4-induced angiogenesis. Matrigels mixed with 1 μg/ml BMP4 or control (*A*), or with 1 μg/ml BMP4 in the presence or absence of noggin (*B*) were injected subcutaneously into 2.5- to 3.5-mo-old $CXXC5^{+/+}$ and $CXXC5^{-/-}$ mice and harvested at d 14 after implantation. Matrigel plugs were subjected to immunohistochemical analyses with an anti-PECAM-1 antibody (green) to observe vascular structures. Nuclei were counterstained with DAPI (blue). Scale bars = 100 μm.

5*C*, bottom panels; *E*; and Supplemental Fig. S3*D*). However, the number of ISAs that reached the dorsal longitudinal anastomotic vessel was not altered in the *cxxc5* morpholino-injected embryos (Fig. 5*C*, *E* and Supplemental Fig. S3*D*). In addition, *cxxc5* morpholino-injected *Tg(flk-1:EGFP)* embryos at 36 hpf showed axial vein-specific induction of endothelial cell apoptosis, as revealed by cleaved caspase 3 staining (Fig. 5*F*, *G* and Supplemental Fig. S3*E*). In HUVECs, *CXXC5* knockdown also increased the number of apoptotic bodies, which were shown by high accumulation of cleaved PARP, a marker of cells undergoing apoptosis (ref. 41 and Supplemental Fig. S3*F*). Thus, CXXC5 is involved in BMP-specific PCV and CVP formation during early zebrafish development.

CXXC5 is required for BMP4-induced angiogenesis *in vivo*

To further characterize the role of CXXC5 in angiogenesis induced by BMP4 *in vivo*, we performed the Matrigel plug assay in $CXXC5^{+/+}$ and $CXXC5^{-/-}$ mice. Matrigel mixed with BMP4 with or without noggin was injected subcutaneously into $CXXC5^{+/+}$ and $CXXC5^{-/-}$ mice. The blood vessels were monitored at d 14 after injection. Microvessel formation in the Matrigel plugs was significantly enhanced by BMP4 treatment in $CXXC5^{+/+}$ mice (Supplemental Fig. S4*A*, right panels show enlarged images of vessels in the plugs). Hematoxylin and eosin staining of the plug sections revealed tube structure of vessels clearly, in which red blood cells were visualized by eosin staining (Supplemental Fig. S4*B*, *C*). However, BMP4-induced microvessel formation in the Matrigel plugs was abolished in $CXXC5^{-/-}$ mice (Supplemental Fig. S4*A*). Furthermore in $CXXC5^{-/-}$ mice, cleaved PARP was increased in the cells migrated into the Matrigel plugs (Supplemental Fig. S4*D*). Immunohistochemical staining of platelet endothelial cell adhesion molecule (PECAM-1), an endothelial cell surface marker (42), more clearly demonstrated BMP4-induced microvessel formation and the absence of this effect in $CXXC5^{-/-}$ mice (**Fig. 6*A***). Furthermore, the presence of noggin or DM inhibited the formation of blood vessels induced by BMP4 in $CXXC5^{+/+}$ mice, as shown by a significant reduction in PECAM-1 staining (Fig. 6*B* and Supplemental Fig. S4*E*). Similar to the results of our *in vitro* analyses, CXXC5 was also induced by BMP4 in the Matrigel plug in $CXXC5^{+/+}$ mice but not $CXXC5^{-/-}$ mice, and this BMP4 effect in $CXXC5^{+/+}$ mice was blocked by noggin (Supplemental

Fig. S4*F*). Thus, CXXC5 is an essential factor for BMP4-induced angiogenesis in mice.

DISCUSSION

Genetic and functional studies have highlighted BMP signaling as a critical pathway regulating endothelial differentiation and vascular development and homeostasis (6). We found that the mRNA level of *Flk-1* increased on treatment with BMP4 or Wnt3a, whereas that of *CXXC5* was increased only by BMP4 treatment, indicating that *CXXC5* induction was specific to BMP signaling. Moreover, the BMP4-induced Flk-1 increment was blocked by BMP signaling inhibitors or *CXXC5* knockdown, while Flk-1 increment induced by CXXC5 overexpression was not inhibited by the BMP signaling inhibitors. These results indicate that CXXC5 functions downstream of BMP signaling.

In this study, we characterized CXXC5 as a transcription factor for *Flk-1* and a mediator of endothelial differentiation by BMP4. First, CXXC5 was found in the nucleus but not in the cytoplasm of mESCs differentiating into endothelial cells. Second, mRNA and promoter activity of *Flk-1* were increased by overexpression of CXXC5 but not by the overexpression of its mutants lacking DNA-binding motif. Furthermore, CXXC5-*Flk-1* promoter interaction was confirmed by DNA binding analyses. We also found that β-catenin levels were not changed by CXXC5 overexpression in HUVECs or mESCs. Overall, CXXC5 is a transcription factor that binds to the *Flk-1* promoter and induces *Flk-1* expression in HUVECs and endothelial-differentiated mESCs.

The BMP signaling stimulates cell migration and tube formation in endothelial cells (43), and we confirmed the roles of CXXC5 in these functions. We further highlighted roles for CXXC5 in cytoskeletal rearrangement and cell migration mediated by BMP4 in endothelial cells. The migration of endothelial cells is essential for sprouting angiogenesis, a complex process involving the sprouting of capillaries from preexisting parent vessels, and the proliferation, migration, and fusion of endothelial cells participating in sprouting angiogenesis are tightly regulated by numerous and specific signals during vessel structure formation (44). In early zebrafish development, sprouting angiogenesis from the DA and PCV are spatiotemporally closed events (45). However, a recent study showed that ISA formation *via* DA sprouting and CVP formation *via* PCV sprouting are specifically activated by VEGF-A and BMP, respectively (13). We found that CXXC5 is specifically expressed in the PCV region of early zebrafish embryos. *cxxc5* knockdown in zebrafish embryo resulted in an aberrant CVP formation but no defects in ISA formation, which mimics the phenotypes previously obtained by the inhibition of BMP signaling in zebrafish embryos (13).

During the sprouting angiogenesis, angiogenic endothelial cells degrade the extracellular matrix to enable their migration and have a high susceptibility to anoikis (45). As a result, these endothelial cells are easily driven to apoptosis when they deviate from the correct location and lose cell survival signals from their surroundings (45). *cxxc5* MO-injected zebrafish embryos showed PCV-specific induction of endothelial cell apoptosis, which may have been caused by inhibition of BMP-induced endothelial cell migration. The role of CXXC5 in angiogenesis was also confirmed by loss of BMP4-induced vessel-like structure formation and the increase of apoptotic cells in the Matrigel plug transplanted into *CXXC5*$^{-/-}$ mice. This evidence demonstrates that CXXC5 acts as a mediator of BMP4-induced *in vivo* endothelial migration and differentiation and angiogenesis.

In summary, we identified CXXC5 as a transcriptional factor activating *Flk-1*, involved in BMP-induced endothelial differentiation. We also characterized CXXC5 as an essential factor mediating BMP-related vessel development in zebrafish. FJ

This work was supported by grants from the National Research Foundation (NRF), funded by the Ministry of Education, Science, and Technology (MEST) of Korea through the Translational Research Center for Protein Function Control (2010-00001919), the Midcareer Researcher Program (2012-010285), and Stem Cell Research Project (2010-0020235); and S.W.S., H.Y.K., M.Y.K., and J.H.Y, were supported by a BK21 studentship from the NRF. The authors thank S. B. Lee for helpful discussions and for sharing unpublished work.

REFERENCES

1. Shibuya, M., and Claesson-Welsh, L. (2006) Signal transduction by VEGF receptors in regulation of angiogenesis and lymphangiogenesis. *Exp. Cell Res.* **312,** 549–560
2. Coultas, L., Chawengsaksophak, K., and Rossant, J. (2005) Endothelial cells and VEGF in vascular development. *Nature* **438,** 937–945
3. Shalaby, F., Rossant, J., Yamaguchi, T. P., Gertsenstein, M., Wu, X. F., Breitman, M. L., and Schuh, A. C. (1995) Failure of blood-island formation and vasculogenesis in Flk-1-deficient mice. *Nature* **376,** 62–66
4. Guo, S., Colbert, L. S., Fuller, M., Zhang, Y., and Gonzalez-Perez, R. R. (2010) Vascular endothelial growth factor receptor-2 in breast cancer. *Biochim. Biophys. Acta* **1806,** 108–121
5. Scott, A., and Mellor, H. (2009) VEGF receptor trafficking in angiogenesis. *Biochem. Soc. Trans.* **37,** 1184–1188
6. Lowery, J. W., and de Caestecker, M. P. (2010) BMP signaling in vascular development and disease. *Cytokine Growth Factor Rev.* **21,** 287–298
7. He, C., and Chen, X. (2005) Transcription regulation of the vegf gene by the BMP/Smad pathway in the angioblast of zebrafish embryos. *Biochem. Biophys. Res. Commun.* **329,** 324–330
8. Park, C., Afrikanova, I., Chung, Y. S., Zhang, W. J., Arentson, E., Fong Gh, G., Rosendahl, A., and Choi, K. (2004) A hierarchical order of factors in the generation of FLK1- and SCL-expressing hematopoietic and endothelial progenitors from embryonic stem cells. *Development* **131,** 2749–2762
9. Suzuki, Y., Montagne, K., Nishihara, A., Watabe, T., and Miyazono, K. (2008) BMPs promote proliferation and migration of endothelial cells via stimulation of VEGF-A/VEGFR2 and angiopoietin-1/Tie2 signalling. *J. Biochem.* **143,** 199–206
10. Goldman, O., Feraud, O., Boyer-Di Ponio, J., Driancourt, C., Clay, D., Le Bousse-Kerdiles, M. C., Bennaceur-Griscelli, A., and Uzan, G. (2009) A boost of BMP4 accelerates the commitment of human embryonic stem cells to the endothelial lineage. *Stem Cells* **27,** 1750–1759
11. Kelly, M. A., and Hirschi, K. K. (2009) Signaling hierarchy regulating human endothelial cell development. *Arterioscler. Thromb. Vasc. Biol.* **29,** 718–724

12. Moreno-Miralles, I., Schisler, J. C., and Patterson, C. (2009) New insights into bone morphogenetic protein signaling: focus on angiogenesis. *Curr. Opin. Hematol.* **16,** 195–201
13. Wiley, D. M., Kim, J. D., Hao, J., Hong, C. C., Bautch, V. L., and Jin, S. W. (2011) Distinct signalling pathways regulate sprouting angiogenesis from the dorsal aorta and the axial vein. *Nat. Cell Biol.* **13,** 686–692
14. Zhang, M., Wang, R., Wang, Y., Diao, F., Lu, F., Gao, D., Chen, D., Zhai, Z., and Shu, H. (2009) The CXXC finger 5 protein is required for DNA damage-induced p53 activation. *Sci. China C Life Sci.* **52,** 528–538
15. Andersson, T., Sodersten, E., Duckworth, J. K., Cascante, A., Fritz, N., Sacchetti, P., Cervenka, I., Bryja, V., and Hermanson, O. (2009) CXXC5 is a novel BMP4-regulated modulator of Wnt signaling in neural stem cells. *J. Biol. Chem.* **284,** 3672–3681
16. Kim, M. S., Yoon, S. K., Bollig, F., Kitagaki, J., Hur, W., Whye, N. J., Wu, Y. P., Rivera, M. N., Park, J. Y., Kim, H. S., Malik, K., Bell, D. W., Englert, C., Perantoni, A. O., and Lee, S. B. (2010) A novel Wilms tumor 1 (WT1) target gene negatively regulates the WNT signaling pathway. *J. Biol. Chem.* **285,** 14585–14593
17. Cokol, M., Nair, R., and Rost, B. (2000) Finding nuclear localization signals. *EMBO Rep.* **1,** 411–415
18. Kalderon, D., Roberts, B. L., Richardson, W. D., and Smith, A. E. (1984) A short amino acid sequence able to specify nuclear location. *Cell* **39,** 499–509
19. Lee, J. H., Voo, K. S., and Skalnik, D. G. (2001) Identification and characterization of the DNA binding domain of CpG-binding protein. *J. Biol. Chem.* **276,** 44669–44676
20. Pendino, F., Nguyen, E., Jonassen, I., Dysvik, B., Azouz, A., Lanotte, M., Segal-Bendirdjian, E., and Lillehaug, J. R. (2009) Functional involvement of RINF, retinoid-inducible nuclear factor (CXXC5), in normal and tumoral human myelopoiesis. *Blood* **113,** 3172–3181
21. Voo, K. S., Carlone, D. L., Jacobsen, B. M., Flodin, A., and Skalnik, D. G. (2000) Cloning of a mammalian transcriptional activator that binds unmethylated CpG motifs and shares a CXXC domain with DNA methyltransferase, human trithorax, and methyl-CpG binding domain protein 1. *Mol. Cell. Biol.* **20,** 2108–2121
22. Aras, S., Pak, O., Sommer, N., Finley, R., Jr., Huttemann, M., Weissmann, N., and Grossman, L. I. (2013) Oxygen-dependent expression of cytochrome c oxidase subunit 4-2 gene expression is mediated by transcription factors RBPJ, CXXC5 and CHCHD2. *Nucleic Acids Res.* **41,** 2255–2266.
23. Yang, D. H., Yoon, J. Y., Lee, S. H., Bryja, V., Andersson, E. R., Arenas, E., Kwon, Y. G., and Choi, K. Y. (2009) Wnt5a is required for endothelial differentiation of embryonic stem cells and vascularization via pathways involving both Wnt/beta-catenin and protein kinase Calpha. *Circ. Res.* **104,** 372–379
24. Park, K. S., Jeon, S. H., Kim, S. E., Bahk, Y. Y., Holmen, S. L., Williams, B. O., Chung, K. C., Surh, Y. J., and Choi, K. Y. (2006) APC inhibits ERK pathway activation and cellular proliferation induced by RAS. *J. Cell Sci.* **119,** 819–827
25. Zeng, L., Xiao, Q., Margariti, A., Zhang, Z., Zampetaki, A., Patel, S., Capogrossi, M. C., Hu, Y., and Xu, Q. (2006) HDAC3 is crucial in shear- and VEGF-induced stem cell differentiation toward endothelial cells. *J. Cell Biol.* **174,** 1059–1069
26. Studier, F. W., Rosenberg, A. H., Dunn, J. J., and Dubendorff, J. W. (1990) Use of T7 RNA polymerase to direct expression of cloned genes. *Methods Enzymol.* **185,** 60–89
27. Lee, W. J., Kim, S. H., Kim, Y. S., Han, S. J., Park, K. S., Ryu, J. H., Hur, M. W., and Choi, K. Y. (2000) Inhibition of mitogen-activated protein kinase by a Drosophila dual-specific phosphatase. *Biochem. J.* **349,** 821–828
28. Matsumoto, T., Bohman, S., Dixelius, J., Berge, T., Dimberg, A., Magnusson, P., Wang, L., Wikner, C., Qi, J. H., Wernstedt, C., Wu, J., Bruheim, S., Mugishima, H., Mukhopadhyay, D., Spurkland, A., and Claesson-Welsh, L. (2005) VEGF receptor-2 Y951 signaling and a role for the adapter molecule TSAd in tumor angiogenesis. *EMBO J.* **24,** 2342–2353
29. Kimmel, C. B., Ballard, W. W., Kimmel, S. R., Ullmann, B., and Schilling, T. F. (1995) Stages of embryonic development of the zebrafish. *Develop. Dynamics* **203,** 253–310
30. Jin, S. W., Beis, D., Mitchell, T., Chen, J. N., and Stainier, D. Y. (2005) Cellular and molecular analyses of vascular tube and lumen formation in zebrafish. *Development* **132,** 5199–5209
31. Passaniti, A., Taylor, R. M., Pili, R., Guo, Y., Long, P. V., Haney, J. A., Pauly, R. R., Grant, D. S., and Martin, G. R. (1992) A simple, quantitative method for assessing angiogenesis and antiangiogenic agents using reconstituted basement membrane, heparin, and fibroblast growth factor. *Lab. Invest.* **67,** 519–528
32. He, T. C., Sparks, A. B., Rago, C., Hermeking, H., Zawel, L., da Costa, L. T., Morin, P. J., Vogelstein, B., and Kinzler, K. W. (1998) Identification of c-MYC as a target of the APC pathway. *Science* **281,** 1509–1512
33. Tetsu, O., and McCormick, F. (1999) Beta-catenin regulates expression of cyclin D1 in colon carcinoma cells. *Nature* **398,** 422–426
34. Cierpicki, T., Risner, L. E., Grembecka, J., Lukasik, S. M., Popovic, R., Omonkowska, M., Shultis, D. D., Zeleznik-Le, N. J., and Bushweller, J. H. (2010) Structure of the MLL CXXC domain-DNA complex and its functional role in MLL-AF9 leukemia. *Nat. Struct. Mol. Biol.* **17,** 62–68
35. Xu, C., Bian, C., Lam, R., Dong, A., and Min, J. (2011) The structural basis for selective binding of non-methylated CpG islands by the CFP1 CXXC domain. *Nat. Commun.* **2,** 227
36. Bai, H., Gao, Y., Arzigian, M., Wojchowski, D. M., Wu, W. S., and Wang, Z. Z. (2010) BMP4 regulates vascular progenitor development in human embryonic stem cells through a Smad-dependent pathway. *J. Cell. Biochem.* **109,** 363–374
37. Nohe, A., Keating, E., Knaus, P., and Petersen, N. O. (2004) Signal transduction of bone morphogenetic protein receptors. *Cell. Signal.* **16,** 291–299
38. Miyazono, K., Kamiya, Y., and Morikawa, M. (2010) Bone morphogenetic protein receptors and signal transduction. *J. Biochem.* **147,** 35–51
39. Heinke, J., Wehofsits, L., Zhou, Q., Zoeller, C., Baar, K. M., Helbing, T., Laib, A., Augustin, H., Bode, C., Patterson, C., and Moser, M. (2008) BMPER is an endothelial cell regulator and controls bone morphogenetic protein-4-dependent angiogenesis. *Circ. Res.* **103,** 804–812
40. Wang, Y. K., Yu, X., Cohen, D. M., Wozniak, M. A., Yang, M. T., Gao, L., Eyckmans, J., and Chen, C. S. (2012) Bone morphogenetic protein-2-induced signaling and osteogenesis is regulated by cell shape, RhoA/ROCK, and cytoskeletal tension. *Stem Cells Dev.* **21,** 1176–1186
41. Oliver, F. J., de la Rubia, G., Rolli, V., Ruiz-Ruiz, M. C., de Murcia, G., and Murcia, J. M. (1998) Importance of poly(ADP-ribose) polymerase and its cleavage in apoptosis. Lesson from an uncleavable mutant. *J. Biol. Chem.* **273,** 33533–33539
42. Yue, W., Pi, Q. M., Zhang, W. J., Zhou, G. D., Cui, L., Liu, W., and Cao, Y. (2010) Platelet endothelial cell adhesion molecule-1, stage-specific embryonic antigen-1, and Flk-1 mark distinct populations of mouse embryonic stem cells during differentiation toward hematopoietic/endothelial cells. *Stem Cells Dev.* **19,** 1937–1948
43. ten Dijke, P., Korchynskyi, O., Valdimarsdottir, G., and Goumans, M. J. (2003) Controlling cell fate by bone morphogenetic protein receptors. *Mol. Cell. Endocrinol.* **211,** 105–113
44. Chappell, J. C., Wiley, D. M., and Bautch, V. L. (2011) Regulation of blood vessel sprouting. *Semin. Cell. Dev. Biol.* **22,** 1005–1011
45. Munoz-Chapuli, R., Quesada, A. R., and Angel Medina, M. (2004) Angiogenesis and signal transduction in endothelial cells. *Cell. Mol. Life Sci.* **61,** 2224–2243
46. Blanc-Brude, O. P., Mesri, M., Wall, N. R., Plescia, J., Dohi, T., and Altieri, D. C. (2003) Therapeutic targeting of the survivin pathway in cancer: initiation of mitochondrial apoptosis and suppression of tumor-associated angiogenesis. *Clin. Cancer Res.* **9,** 2683–2692
47. Wan, C., Gilbert, S. R., Wang, Y., Cao, X., Shen, X., Ramaswamy, G., Jacobsen, K. A., Alaql, Z. S., Eberhardt, A. W., Gerstenfeld, L. C., Einhorn, T. A., Deng, L., and Clemens, T. L. (2008) Activation of the hypoxia-inducible factor-1alpha pathway accelerates bone regeneration. *Proc. Natl. Acad. Sci. U. S. A.* **105,** 686–691

Received for publication June 17, 2013.
Accepted for publication October 7, 2013.